Controlled electron transport in coupled Aharonov-Bohm rings

Supriya Jana and Arunava Chakrabarti[†]

Department of Physics, University of Kalyani, Kalyani, West Bengal-741 235, India.

Abstract

We propose a simple model of two coupled mesoscopic rings threaded by magnetic flux which mimics a device for electron transmission in a controlled fashion. Within a tight binding formalism we work out exactly the conditions when a completely ballistic transmission can be triggered at any desired position of the Fermi level within a continuous range of energy. The *switching* action can be easily controlled by appropriately tuning the values of the flux through the two rings. The general transmission across the ring system displays interesting features characterized by the appearance and collapse of Fano resonances, and the supression of the Aharonov-Bohm oscillations in several casess. We report and analyze exact analytical results for a few such cases.

[†]**Electronic mail**: arunava_chakrabarti@yahoo.co.in

1. Introduction

The study of electronic conductance in mesoscopic rings threaded by a magnetic flux has been an important and extensively studied field for many years [1]-[5]. With the experimental realization of mesoscopic rings and cylinders [6]-[8] and later, the quantum dots and quantum wires [9]-[12], the research in this field got the desired momentum. Present day nanofabrication and lithographic techniques have enabled us to study the effects of quantum coherence in small scale systems and to explore the possibility of controlling electronic transport in tailor made devices [13]-[14].

In recent years one witnesses a large number of theoretical works which focus on the basics of quantum transport in low dimensional systems using very simple tight binding models [15]-[23]. The models find their justification in the state of the art mesoscopic and nanotechnology where using the tip of a scanning tunnel microscope (STM) one can literally build up an atomic wire [16, 17] or an array of quantum dots with a desired geometry. Interestingly enough, even studies with non-interacting electrons have been found to produce results which in many cases bring out the essential qualitative features of the real-life systems and at the same time throws light into the basics of quantum transport in quasi-one dimension [18]- [21].

In this communication we address the problem of electron transport across a model mesoscopic ring (the Primary ring) which is coupled at one point to a 'secondary' ring. Both the rings contain magnetic flux perpendicular to the plane of the rings. The basic motivation behind the present work is to look for a comprehensive control over the transmission across a mesoscopic ring by an atomic cluster attached to it from one side. To our mind, inspite of the existing studies there is ample scope to explore the role of an external magnetic field in gaining control over electronic transmission in closed loop geometries, and in designing a switching device even using rings with minimal sizes. We get quite inspiring results. For example, we show that even with a minimum number of atomic sites contained in the rings, the system offers a very efficient way of controlling electron transport that can be tuned at will by mutually adjusting the magnetic field and the inter-ring coupling. In particular, a sharp *switch action* can be triggered at *any position of the Fermi level* within a given range. This can be quite important from the standpoint of designing

a quantum tunnel device. In addition to this, interesting Aharonov-Bohm (AB) oscillations [24] as well as the supression of AB oscillations as a function of the inter-ring coupling parameter are observed. Fano lineshapes [25] are observed in the transmission spectrum which can be made to collapse and even disappear by controlling the secondary flux.

In what follows we present the results of our analysis. In Section 1 we describe the model. The switch action and the transmission profiles are presented in section 2. In section 3 we analyse the appearance of the Fano lineshapes and in Section 4 we draw conclusions.

2. The Model and the method

Let us begin by refering to Fig.1(a). The 'primary' ring (P) contains a total of $l + 2m + 1$ sites and is coupled to the secondary ring (S) which contains $N + 1$ sites. The contact point is marked by the site μ, and the P-S hopping integral is λ. A magnetic flux Φ_P threads the primary ring, while the flux through the secondary ring is Φ_S. Two semi-infinite perfect leads are connected to the primary ring at the end-points A and B as shown. The hamiltonian, in the tight binding approximation, for the lead(L)-ring-lead system is given by,

$$H = H_L + H_P + H_S + H_{P-S} + H_{P-L} \tag{1}$$

where,

$$
\begin{aligned}
H_L &= \epsilon_0 \sum_{i=-\infty}^{A-1} c_i^\dagger c_i + \epsilon_0 \sum_{i=B+1}^{\infty} c_i^\dagger c_i + t_0 \sum_{<ij>} c_i^\dagger c_j + h.c. \\
H_P &= \epsilon_A c_A^\dagger c_A + \epsilon_B c_B^\dagger c_B + \epsilon_0 \left(\sum_{i \in \mathcal{U}} c_{i,P}^\dagger c_{i,P} + \sum_{i \in \mathcal{L}} c_{i,P}^\dagger c_{i,P} \right) + t_0 \exp(i\theta_P) \sum_{<ij>} c_{i,P}^\dagger c_{j,P} + h.c. \\
H_S &= \epsilon_0 \sum_{i=1}^{N} c_{i,S}^\dagger c_{i,S} + t_0 \exp(i\theta_S) \sum_{<ij>} c_{i,S}^\dagger c_{j,S} + h.c. \\
H_{P-S} &= \lambda c_{\mu,\mathcal{L}}^\dagger c_{1,S} \\
H_{P-L} &= t_0 (c_A^\dagger c_{A-1} + c_B^\dagger c_{B+1}) \tag{2}
\end{aligned}
$$

In the above, $c_i^\dagger (c_i)$ represents the creation (annihilation) operator for the leads, the ring and

3

the QD chain at the appropriate sites. The symbols P or S in Eq.(1) as well as in the subscripts in Eqs.(2) represent the primary or the secondary ring in repective order. $\mathcal{U}$ and $\mathcal{L}$ symbolize the upper and the lower arms of the primary rings. order. The on-site potential at the leads, at the edges A and B, and in the bulk of the rings are all taken to be ϵ_0 including the site marked μ. So, we are primarily interested in the effect of the geometry on the transport properties. The amplitude of the hopping integral is taken to be t_0 throughout except the hopping from the site μ in the ring to the first site of the QD chain, which has been symbolized as λ and represents the 'strength' of coupling between the rings P and S. θ_P and θ_S are given by $\theta_P = 2\pi\Phi_P/(l+2m+1)\Phi_0$, and $\theta_s = 2\pi\Phi_S/(N+1)\Phi_0$ respectively, where, $\Phi_{P(S)}$ is the flux threading the primary (secondary) ring and $\Phi_0 = hc/e$ is the fundamental flux quantum. The task of solving the Schrödinger equation to obtain the stationary states of the system can be reduced to an equivalent problem of solving a set of difference equations. We list the relevant equations below.

For the sites A and B at the ring-lead junctions,

$$
\begin{aligned}
(E - \epsilon_A)\psi_A &= t_0 e^{i\theta_P}\psi_{1,\mathcal{U}} + t_0 e^{-i\theta_P}\psi_{1,\mathcal{L}} + t_0\psi_{A-1} \\
(E - \epsilon_B)\psi_B &= t_0 e^{-i\theta_P}\psi_{l,\mathcal{U}} + t_0 e^{i\theta_P}\psi_{2m+1,\mathcal{L}} + t_0\psi_{B+1}
\end{aligned}
$$

$$(3)$$

In the above, ψ_{A-1} and ψ_{B+1} represent the amplitudes of the wave function at the sites on the lead which are closest to the points A and B, and, $\mathcal{U}$ and $\mathcal{L}$ in the subscripts refer to the 'upper' and the 'lower' arms of the primary ring respectively.

For the sites in the bulk of the primary ring the equations are,

$$
\begin{aligned}
(E - \epsilon_0)\psi_{j,\mathcal{U}} &= t_0 e^{-i\theta_P}\psi_{j-1,\mathcal{U}} + t_0 e^{i\theta_P}\psi_{j+1,\mathcal{U}} \\
(E - \epsilon_0)\psi_{j,\mathcal{L}} &= t_0 e^{i\theta}\psi_{j-1,\mathcal{L}} + t_0 e^{-i\theta_P}\psi_{j+1,\mathcal{L}}
\end{aligned}
$$

$$(4)$$

and, for the site marked μ in the lower arm of the ring, the equation is,

$$(E - \epsilon_0)\psi_{\mu,\mathcal{L}} = t_0 e^{i\theta_P}\psi_{\mu-1,\mathcal{L}} + t_0 e^{-i\theta_P}\psi_{\mu+1,\mathcal{L}} + \lambda\psi_{1,S} \tag{5}$$

4

$\mu \pm 1$ implying the sites to the right and to the left of the site marked μ respectively. Finally, for the sites in the secondary ring we have the following set of equations,

$$
\begin{aligned}
(E - \epsilon_0)\psi_{1,S} &= \lambda\psi_\mu + t_0 e^{i\theta_S}\psi_{2,S} + t_0 e^{-i\theta_S}\psi_{N,S} \\
(E - \epsilon_0)\psi_{2,S} &= t_0 e^{i\theta_S}\psi_{3,S} + t_0 e^{-i\theta_S}\psi_{1,S} \\
&\quad . \\
&\quad . \\
(E - \epsilon_0)\psi_{N,S} &= t_0 e^{i\theta_S}\psi_{1,S} + t_0 e^{-i\theta_S}\psi_{N-1,S} \quad (6)
\end{aligned}
$$

where the central set of equations above refer to the bulk sites viz. $j = 2, ...N - 1$ in the QD array

To calculate the transmission coefficient across such a coupled ring system we adopt the following steps. First, the dangling S-ring is 'wrapped' up into an effective site by decimating the amplitudes $\psi_{2,S}$ to $\psi_{N,S}$ in the secondary ring. The renormalized on-site potential of the first site of the S-ring is given by,

$$
\epsilon^* = \epsilon_0 + \frac{2t_0^2(E - \epsilon')}{\Delta} + \frac{2t_0^3}{\Delta U_{N-2}(x)}\cos(2\pi\Phi_S/\Phi_0) \quad (7)
$$

where,

$$
\begin{aligned}
\epsilon' &= \epsilon_0 + \frac{t_0 U_{N-3}(x)}{U_{N-2}(x)} \\
\Delta &= (E - \epsilon')^2 - \frac{t_0^2}{U_{N-2}^2(x)} \quad (8)
\end{aligned}
$$

In the above equations, $x = (E - \epsilon_0)/2t_0$ and $U_j(x)$ is the jth order Chebyshev polynomial of the second kind, with $U_0 = 1$ and $U_{-1} = 0$. The bulk sites of the primary ring are then decimated to convert the P-S ring system into an effective 'diatomic molecule' $A - B$ clamped between the leads (Fig.1(b)). The effective on-site potentials at A and B and the renormalized

5

flux dependent hopping integral between them are given by [26],

$$\sigma_{A(B)} = \epsilon_0 + t_0 \left[\frac{U_{l-1}}{U_l} + \frac{U_{m-1}}{U_m} \right] + \left(\frac{t_0}{U_m} \right)^2 \chi(E, \lambda, \Phi_S)$$

$$t_F = \frac{t_0}{U_l} e^{i\theta_P(l+1)} + \frac{t_0^2}{U_m^2} \chi(E, \lambda, m) e^{-i(2m+2)\theta_P} \tag{9}$$

where, $\chi(E, \lambda, m) = [E - \omega - 2t_0 U_{m-1}/U_m]^{-1}$, with $\omega = \epsilon_0 + \lambda^2/(E - \epsilon^*)$. The two-terminal transmission coefficient across the primary ring is given by [27],

$$T = \frac{4 \sin^2 qa}{|M_{12} - M_{21} + (M_{11} - M_{22}) \cos qa|^2 + |M_{11} + M_{22}|^2 \sin^2 qa} \tag{10}$$

Here, a is the lattice spacing in the leads, taken as unity throughout. $q = \cos^{-1}[(E - \epsilon_0)/2t_0]$ is the wave vector. The Transfer matrix elements are given by, $M_{11} = (E - \sigma_A)(E - \sigma_B)/(t_0 t_F) - t_B/t_0$; $M_{12} = -(E - \sigma_B)/t_F$; $M_{21} = (E - \sigma_A)/t_F$, and $M_{22} = -t_0/t_F$.

3. Results and discussions

(a) The switch action

We first discuss the principal result of the present work, i.e. how can such a system of coupled rings be used to trigger ballistic transmission at any desired energy within a given range. To make things less obscure, we concentrate on the simplest situation where, the primary (P) ring contains four sites (the sites at A, B, and one site in each arm), and the secondary (S) ring has just three sites. We call such a system a $(4, 3)$ system. The effective on-site potential ϵ^* in this case is given by,

$$\epsilon^* = \epsilon_0 + \frac{2t_0^2(E - \epsilon_0)}{\Delta} + \frac{2t_0^3}{\Delta} \cos 3\theta_S \tag{11}$$

where, $\Delta = (E - \epsilon_0)^2 - t_0^2$. It is known [26] that, for a primary flux $\Phi_P = \Phi_0/2$, such a system exhibits a ballistic transmission at $E = \epsilon^*$ which, in the present case leads to an equation, $\cos 3\theta_S = F(E)$, where,

$$F(E) = \frac{E - \epsilon_0}{2t_0^3} \left[(E - \epsilon_0)^2 - t_0^2 \right] \tag{12}$$

Eq.(12) implies that, for the entire range of energy for which $F(E)$ remains bounded by ± 1, one can easily fix up a value of the secondary flux Φ_S such that the transmission across the primary ring is unity, as discussed elsewhere [26]. In the simple case of the $(4, 3)$ system, the function $F(E)$ remains within ± 1 for all values of the energy E within $(\epsilon_0 - 2t_0, \epsilon_0 + 2t_0)$, i.e. for the entire allowed band of the semi-infinite ordered leads. This is illustrated in Fig.2. Thus, the $(4, 3)$ system can be tuned by the secondary flux to act as a switch corresponding to any desired position of the Fermi level within the said range. For example, with $\epsilon_0 = 0$ and, $t_0 = 1$, if we set the Fermi level at $E = 1$, then a ballistic transmission $(T = 1)$ is obtained by setting $\Phi_S = \Phi_0/2$. The transmission at all other values of the secondary flux remains zero. This is what we mean by a *switch action*. For energy values other than $E = 1$ we get a couple of values of Φ_S placed symmetrically around $\Phi_S = \Phi_0/2$. Interestingly, as one approaches the value $E = 1$, the separation between the two values of the secondary flux which correspond to the resonant transmission get reduced smoothly, and finally, at $E = 1$ the pair of peaks collapse to give a single sharp resonance peak in the transmission spectrum. This aspect is depicted in Fig.3. The appearance of a single resonance peak at $E = 1$ can be understood easily by analyzing the expression of ϵ^*.

Before we end this section it should be pointed out that, the switch action is strongly dependent on making the effective hopping across the vertices $A - B$ in the primary ring. This can be achieved whenever one has an equal number of scatterers in the upper and the lower arms of the primary ring, and sets $\Phi_P = \Phi_0/2$. We have also investigated many cases when the secondary ring contains more than just three atoms. As long as the selected energy (the Fermi energy) is chosen to be within the spectrum of the secondary ring (and also within the allowed band of the leads), there will be a switch action. Hence, the result presented for the $(4, 3)$ case is perfectly general, and really can be achieved independent of the size of the rings when one tunes the hamiltonian parameters appropriately.

(b) Fano lineshape in the transmission spectrum:

Fano lineshape [25] in the transmission is widely displayed by several mesoscopic systems [23].

This typical resonance profile is observed when a discrete, bound level get 'mixed' with a continuum of states. Atomic clusters dangling from a linear chain provide such an example [28, 29], and the present case is no exception. However, in this case interesting changes in the Fano lineshapes in the transmission spectrum take place as the flux through the secondary ring is varied keeping the primary flux fixed. The opposite is also true, but we report just one case, viz, the effect of variation of the seconadry flux, to save space. To this end, we have analyzed in some details the transmission amplitude for the $(4, 3)$ system for particular values of the energy E in the δ-neighborhood of a transmission minimum (as the secondary flux is varied). The transmission amplitude, apart from a phase factor, is given by,

$$\tau \sim 2 \sin q \frac{G_2 \delta + \frac{F_2}{G_2}}{F_4 (\delta + \frac{G_4}{F_4}) + i F_5 (\delta + \frac{G_5}{F_5})} \tag{13}$$

where, $F_5 = -F_2 F_3 + G_2 G_3 + 2 G_1 \cos q$; $G_5 = G_3 F_2 - 2(E - F_1) \cos q - t_0$; $F_4 = (G_3 G_2 - F_3 F_2 - G_1) \sin q$; $G_4 = (E - F_1 + F_2 G_3) \sin q + t_0 \sin 2q$; $F_3 = [2 G_1 (E - F_1) + G_2^*]/t_0$; $G_3 = [(E - F_1)^2 - F_2^*]/t_0$; $F_2 = t_0^2 \exp(2i\theta_P)/(E - \epsilon_0) + x \exp(-2i\theta_P)/y$; $G_2 = (z - b/(E - a)) x \exp(-2i\theta_P)/y$; $F_1 = \epsilon_0 + t_0^2/(E - \epsilon_0) + x/y$; $G_1 = x(z - b/(E - a))/y$; $x = t_0^2 (E - a)$; $y = (E - \epsilon_0)(E - a) - \lambda^2$ and $z = b(E - \epsilon_0)/y$.

The asymmetry parameter [29, 30] is given by F_2/G_2, which is, in general, complex in the present geometry. The numerator of Eq.(13) is zero when $\delta = -F_2/G_2$, while the real part of the denominator vanishes for $\delta = -G_4/F_4$. These *de-tuned* zeros give rise to an asymmteric Fano profile [30] around the secondary flux $\Phi_S = \Phi_S^{min}$, Φ_S^{min} is the secondary flux corresponding to the transmission minimum in Fig.4. The sign of the quantity $Q = (F_2/G_2 - G_4/F_4)$ is responsible for whether the Fano lineshape exhibits a *peak to dip* drop in the transmission or a sharp *dip to peak* rise in it. It is simple to check that the sign of Q changes as one the secondary flux from $\Phi_S = \Phi_0/2 - \Phi_S^{min}$ to $\Phi_S = \Phi_0/2 + \Phi_S^{min}$. This swapping of the Fano profile is clearly visible in Fig.4 where we have plotted the transmission coefficient as a function of the secondary flux when the primary flux is quite arbitrarily fixed $\Phi_P = \Phi_0/5$. We have taken the P-S coupling $\lambda = 0.08 t_0$, a weak one. For strong coupling, the Fano resonances become broadened as λ controls the width of resonance. As the energy is gradually changed from $E = 0$

8

to $E = 1$, interestingly we observe that, while for $E = 0$ the Fano like behaviour is obscure (the transmission coefficient appears as delta-like peaks only), with increasing energy the asymmetric Fano profile is clearly visible and the lineshape swaps from a *dip-to-peak* to a *peak-to-dip* pattern as the secondary flux crosses the half flux quantum mark. In addition to this, the gap between the Fano anti-resonances shrinks as one approaches the value $E = 1$, and finally disappears completely at $E = 1$ (not shown in this picture). This latter observation is easily justified from Eq.(11). The features exhibited in Fig.4 are also observed even if we set the primary flux equal to zero.

The effect of the P-S coupling λ on the transmission spectrum has also been studied in details. Apart from controlling the width of the lineshape, an increasing λ can suppress the AB oscillations as shown in Fig.5. Here, we present the results for $E = 0$ and the primary flux set equal to the half flux quantum. The overall transmission enhances as λ is increased, reaching alsmost unity as the inter-ring coupling becomes sufficiently large. This gives us an idea of the effect of the proximity of the primary and the secondary rings.

4. Conclusions

A coupled ring system can exhibit a wealth of transmission characteristics as the magnetic flux threading the rings are adjusted. We have focussed on certain specific issues, one of which is the possibility of a ballistic transport at any desired value of the Fermi energy that can be controlled by tuning the secondary flux. This gives the coupled ring system the status of a *mesoscopic switch* which can be put 'on' at will. Fano lineshapes are observed in the transmission spectrum under various occasions and we have analyzed one such case where the Fano profile swaps as the secondary flux changes. Finally, the collapse of the Aharonov-Bohm oscillations as the inter-ring coupling increases is also discussed.

References

[1] N. Byers and C. N. Yang, Phys. Rev. Lett. 7 (1961) 46.

[2] B. L. Al'tshuler, A. G. Aronov and B. Z. Spivak, JETP Lett. 33 (1981) 94.

[3] M. Büttiker, Y. Imry and R. Landauer, Phys. Lett. A 96 (1983) 365.

[4] Y. Imry, J. Phys. C 15 (1982) L221.

[5] J. L. D'Amato, H. M. Pastawski and J. F. Weisz, Phys. Rev. B 39 (1989) 3554.

[6] D. Yu Sharvin and Yu. V. Sharvin, JETP Lett. 34 (1981) 273.

[7] B. L. Al'tshuler, A. G. Aronov. B. Z. Sivak, D. Yu Sharvin and Yu. V. Sharvin, JETP Lett. 35 (1982) 589.

[8] M. Gijs, C. Van Haesendonck and Y. Bruynseraedl, Phys. Rev. Lett. 52 (1984) 2069.

[9] V. V. Mitin, V. A. Kochelap and M. A. Stroscio, Quantum Heterostructures, Cambridge University Press (1999).

[10] Y. Aharonov and D. Bohm, Phys. Rev. 115 (1959) 485.

[11] A. Levy Yeyati and M. Büttiker, Phys. Rev. B 52 (1995) R14360.

[12] D. K. Ferry and S. M. Goodnick, Transport in Nanostructures, Cambridge University Press (1997).

[13] N. Sundaram, S.A. Chalmers, P. F. Hopkins and A. C. Gossard, Science 254 (1991) 1326.

[14] P. Gambardealla, M. Blanc, H. Brune, K. Kuhnke and K. Kern, Phys. Rev. B 61 (2000) 2254.

[15] J. O. Vasseur, P. A. Deymier, L. Dobrzynski and J. Choi, J. Phys. Condens. Matter, 10 (1998) 8973.

[16] V. Pouthier and C. Girardet, Phys. Rev. B 66 (2002) 115322.

[17] J. M. Cerveró and A. Rodríguez, Phys. Rev. A 70 (2004) 052705.

[18] Ji-R. Shi and B. Y. Gu, Phys. Rev. B 55 (1997) 4703.

[19] F. Domínguez-Adame, I. Gómez, P. A. Orellana and M. L. Ladrón de Guevara, Microelectron. J. 35 (2004) 87.

[20] P. A. Orellana, M. L. Ladrón de Guevara and F. Claro, Phys. Rev. B 70 (2004) 233315.

[21] L. E. F. Foa Torres, H. M. Pastawski and E. Medina, Europhys. Lett. 73 (2006) 164.

[22] P. A. Orellana, F. Domínguez-Adame, I. Gómez, M. L. Ladrón de Guevara, Phys. Rev. B 67 (2003) 085321.

[23] A. Rodríguez, F. Domínguez-Adame, I. Gómez, P. A. Orellana, Phys. Lett. A 320 (2003) 242.

[24] Y. Aharonov and D. Bohm, Phys. Rev. 115 (1959) 485.

[25] U. Fano, Phys. Rev. 124 (1961) 1866.

[26] S. Jana and A. Chakrabarti, Phys. Rev. B 77 (2008) 155310.

[27] A. Douglas Stone, J. D. Joannopoulos, D. J. Chadi, Phys. Rev. B 24 (1981) 5583.

[28] A. Miroshnichenko, Y. Kivshar, Phys. Rev. E 72 (2005) 056611.

[29] A. Chakrabarti, Phys. Lett. A 366 (2007) 507; Phys. Rev. B 74 (2006) 205315.

[30] K.-K. Voo, C. S. Chu, Phys. Rev. B 72 (2005) 165307.
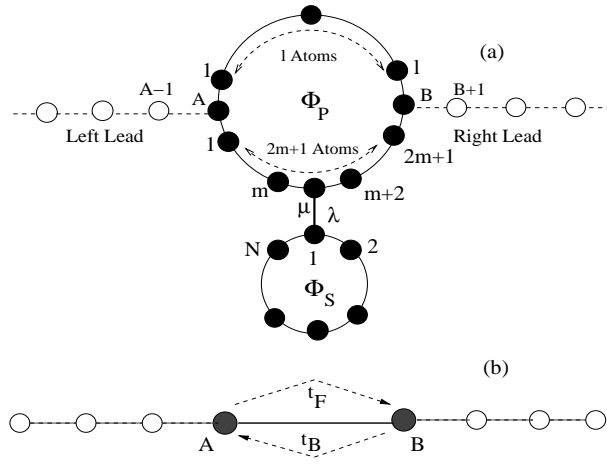
Figure Captions:

Figure 1: (a) Schematic representation of the coupled ring system, and (b) renormalization of the ring system into a 'diatomic molecule'.

Figure 2: $F(E)$ versus E curve for the $(4, 3)$ ring system. We have chosen $\epsilon_0 = 0$, $t_0 = 1$ everywhere, and E is measured in unit of t_0.

Figure 3: Transmission across a $(4, 3)$ coupled ring system with $\lambda = 0.2 t_0$. Here, $E = 0.5$ (solid), 0.75 (dashed) and 1.0 (dotted) measured in unit of t_0. $\Phi_P = \Phi_0/2$ and the other parameters are same as in the previous figures.

Figure 4: Fano profiles in the transmission spectrum of a $(4, 3)$ coupled ring system. We have taken $\Phi_P = \Phi_0/5$, $\lambda = 0.08 t_0$ and $E = 0$ (solid line), 0.2 (dashed line) $and 0.75 (dotted line)$ mesured in unit of t_0. ϵ_0 and t_0 are as in Fig.2.

Figure 5: Collapse of the AB oscillations as the inter-rine coupling λ is increased. We have fixed $\Phi_P = \Phi_0/2$ and $E = 0$. $\lambda = 0.25$ (solid), 1.0 (dashed), 3.0 (dotted) and 5.0 (thick) in unit of t_0. ϵ_0 and t_0 are chosen as zero and unity as before.

Figure 1: (a) Schematic representation of the coupled ring system, and (b) renormalization of the ring system into a 'diatomic molecule'.
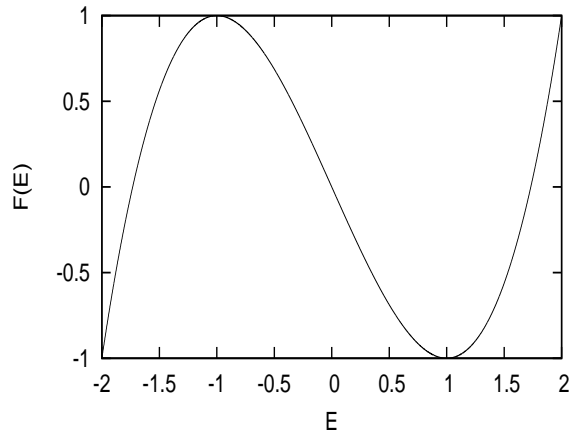
Figure 2: $F(E)$ versus E curve for the $(4, 3)$ ring system. We have chosen $\epsilon_0 = 0$, $t_0 = 1$ everywhere, and E is measured in unit of t_0.
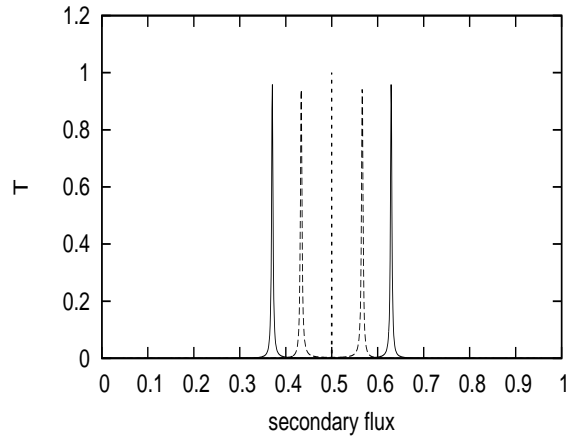
Figure 3: Transmission across a $(4, 3)$ coupled ring system with $\lambda = 0.2t_0$. Here, $E = 0.5$ (solid), 0.75 (dashed) and 1.0 (dotted) measured in unit of t_0. $\Phi_P = \Phi_0/2$ and the other parameters are same as in the previous figures.
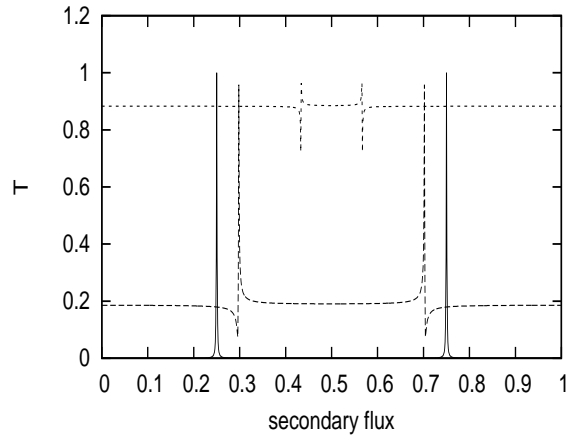
15

Figure 4: Fano profiles in the transmission spectrum of a $(4, 3)$ coupled ring system. We have taken $\Phi_P = \Phi_0/5$, $\lambda = 0.08t_0$ and $E = 0$ (solid line), 0.2 (dashed line) and 0.75 (dotted line) mesured in unit of t_0. ϵ_0 and t_0 are as in Fig.2.
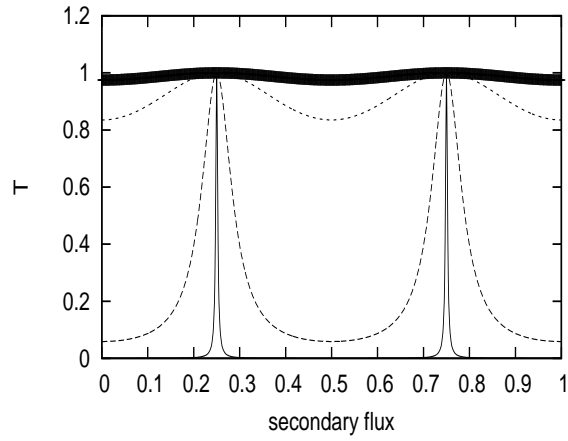
Figure 5: Figure 5: Collapse of the AB oscillations as the inter-rine coupling λ is increased. We have fixed $\Phi_P = \Phi_0/2$ and $E = 0$. $\lambda = 0.25$ (solid), 1.0 (dashed), 3.0 (dotted) and 5.0 (thick) in unit of t_0. ϵ_0 and t_0 are chosen as zero and unity as before.